Improved full-range equivalent circuit and energy balance of the dynamo type flux pump

Antonio Morandi, Giacomo Russo , Massimo Fabbri and Luca Soldati

LIMSA – Laboratory of Magnet Engineering and Applied Superconductivity

University of Bologna, Italy

Dep. of Electrical, Electronic and Information Engineering

Wednesday, June 23, 2021

8th International Workshop on Numerical Modelling of High Temperature Superconductors
14th – 16th June 2022, Nancy, France

Outline

- Motivation and case study
  - ✓ Geometric parameters, assumptions, types of load
- The FEM model of the FP based on the Volume Integral Equations approach
  - ✓ Discretization and solving system, FEM based equivalent circuit, Energy balance and efficiency
- Numerical results, equivalent circuits and their limits
  - ✓ Operation with impressed DC current – V-I characteristic and energy balance
  - ✓ Partial and complete equivalent circuit
  - ✓ Static and transient analysis (charging of RL load)
- Conclusion

HTS (dynamo) flux pump – some references

[1] C. Hoffmann, D. Pooke e A. D. Caplin, «Flux Pump for HTS Magnets,» IEEE Transactions on Applied Superconductivity, vol. 21, n. 3, June 2011.
[2] Zhenan Jiang, K. Hamilton, Naoyuki Amemiya, R. A. Badcock, and C. W. Bumby , "Dynamic resistance of a high-Tc superconducting flux pump", Appl. Phys. Lett. 105, 112601 (2014).
[3] Jiang, Z., Bumby, C.W., Badcock, R.A., (...), Long, N.J., Amemiya, N., Impact of flux gap upon dynamic resistance of a rotating HTS flux pump, 2015, SUST, 28(11)
[4] Jiang, Z., Bumby, C.W., Badcock, R.A., ..., Park, M., A rotating flux pump employing a magnetic circuit and a stabilized coated conductor HTS stator Journal of Magnetics, 2016, 21(2)
[5] C. W. Bumby, A. E. Pantoja, H. Sung, Z. Jiang, R. Kulkarni and R. A. Badcock, "Through-Wall Excitation of a Magnet Coil by an External-Rotor HTS Flux Pump," in IEEE Transactions on Applied Superconductivity, vol. 26, no. 4, pp. 1-5, June 2016, Art no. 050.
[6] Chris W Bumby, Rodney A Badcock, Hae-Jin Sung, Kwang-Min Kim, Zhenan Jiang, Andres E Pantoja , Patrick Bernardo, Minwon Park and Robert G Buckley ,Development of a brushless HTS exciter for a 10 kW HTS synchronous generator.
[7] L. Fu, K. Matsuda, T. Lecrevisse, Y. Iwasa e T. Coombs, «A flux pumping method applied to the magnetization of YBCO superconducting coils: frequency, amplitude and waveform characteristics,» Superconductor Science and Technology, 2016.
[8] W. Wang, Y. Lei, S. Huang, P. Wang, Z. Huang e Q. Zhou, «Charging 2G HTS Double Pancake Coils With a Wireless Superconducting DC Power Supply for Persistent Current Operation,» IEEE Transactions on Applied Superconductivity, vol. 28, n. 3, April 2018.
[9] Y. Zhang, W. Wang, H. Ye, X. Wang, Y. Gao, Q. Zhou, X. Liu e Y. Lei, «Compact Linear-Motor Type Flux Pumps With Different Wavelengths for High-Temperature Superconducting Magnets,» IEEE Transactions on Applied Superconductivity, vol. 30, n. 4, June 2020.
[10] Geng, Jianzhao, et al. "Origin of dc voltage in type II superconducting flux pumps: field, field rate of change, and current density dependence of resistivity."Journal of Physics D: Applied Physics 49.11 (2016): 11LT01.
[11] T. A. Coombs, «Superconducting flux pumps,» Journal of Applied Physics, 2019.
[12] T. A. Coombs, J. Geng, L. Fu e K. Matsuda, «An Overview of Flux Pumps for HTS Coils,» IEEE Transactions on Applied Superconductivity, vol. 27, n. 4, June 2017.
[13] R. C. Mataira, M. D. Ainslie, R. A. Badcock e C. W. Bumby, Origin of the DC output voltage from a high-Tc superconducting dynamo, Applied Physics Letters, April 2019.
[14] M. Ainslie, F. Grilli, L. Quéval, E. Pardo, F. Perez-Mendez, R. Mataira, A. Morandi, A. Ghabeli, C. Bumby e R. Brambilla, «A new benchmark problem for electromagnetic modelling of superconductors: the high-Tc superconducting dynamo,» Superconductor Science and Technology, August 2020.
[15] A. Ghabeli e E. Pardo, «Modeling of airgap influence on DC voltage generation in a dynamo-type flux pump,» Superconductor Science and Technology, 2020.
[16] R. Mataira, M. D. Ainslie, R. Badcock e C. W. Bumby, «Modeling of stator versus magnet width effects in high-Tc superconducting dynamos,» IEEE TASC, 2020.
[17] M. D. Ainslie, L. Quéval, R. C. Mataira e C. W. Bumby, Modelling the frequency dependence of the open-circuit voltage of a high-Tc superconducting dynamo, IEEE TASC, 2021.
[18] Ghabeli, A., Pardo, E. & Kapolka, M. 3D modeling of a superconducting dynamo-type flux pump. Sci Rep 11, 10296 (2021). https://doi.org/10.1038/s41598-021-89596-4
[19] Asef Ghabeli, Mark Ainslie, Enric Pardo, Loïc Quéval and Ratu Mataira, Modeling the charging process of a coil by an HTS dynamo-type flux pump, SUST, 34(8)
[20] Mataira, Ratu, et al. "Mechanism of the high-T c superconducting dynamo: models and experiment."Physical Review Applied14.2 (2020): 024012.
[21] J.Geng,B.Shen,C.Li,H.Zhang,K.Matsuda,J.Li,X.Zhang,T.Coombs “Voltage-ampere characteristics of YBCO coated conductor under inhomogeneous oscillating magnetic field” Appl. Phys. Lett.,108(26)(2016)
[22] Z. Jiang, C. W. Bumby, R. A. Badcock, N. J. Long, H. J. Sung, and M. Park, “A Rotating Flux Pump Employing a Magnetic Circuit and a Stabilized Coated Conductor HTS Stator,” Journal of Magnetics, vol. 21, no. 2. The Korean Magnetics Society, pp. 239–243, 30-Jun-2016
[23] A Morandi, G Russo, M Fabbri and L Soldati, Energy balance, efficiency and operational limits of the dynamo type flux pump, 2022, SUST, 35(6)
[24] Wen Z, Zhang H, Mueller M. High Temperature Superconducting Flux Pumps for Contactless Energization. *Crystals*. 2022; 12(6):766

HTS dynamo flux pump technology - status and applications

- **A DC voltage is produced at the terminals of a dynamo flux pump device, in which a superconducting tape is exposed to a travelling magnetic field produced by a permanent magnet (or more) that cyclically passes on it.**
- **This counterintuitive and widely debated effect has been widely confirmed by experiments.**

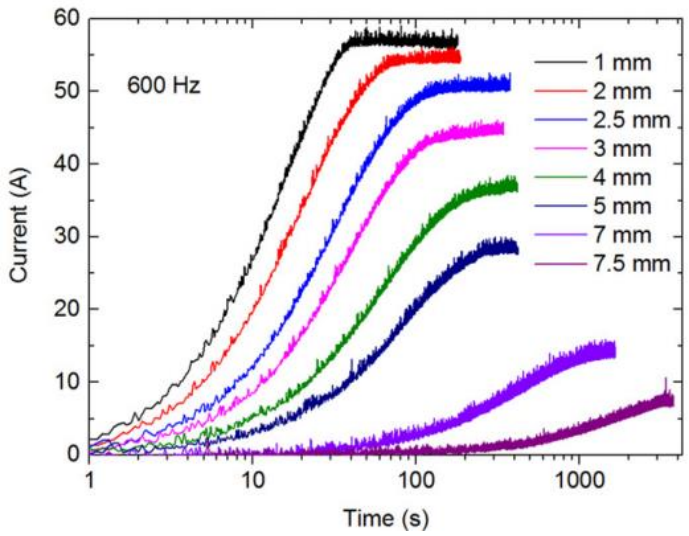

Plateau current

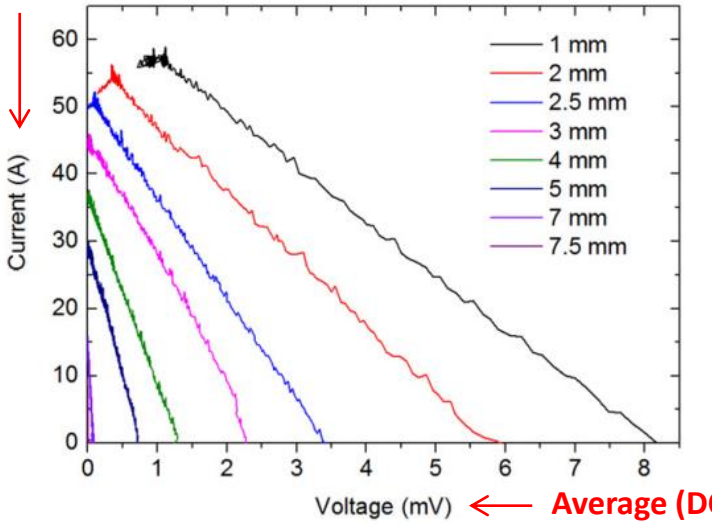

Average (DC) voltage

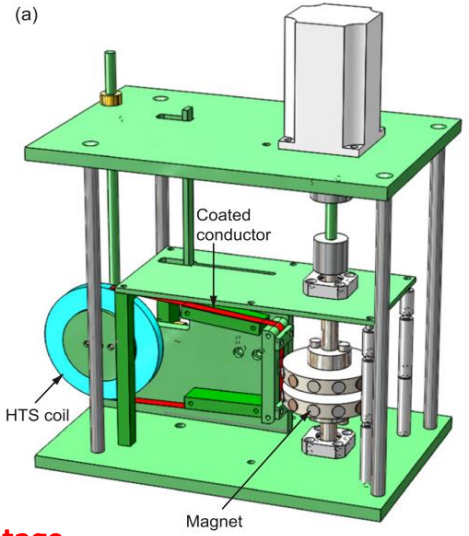

Jiang, Z., Bumby, C.W., Badcock, R.A., (...), Long, N.J., Amemiya, N., Impact of flux gap upon dynamic resistance of a rotating HTS flux pump, 2015, SUST, 28(11)

- **HTS (dynamo) Flux pump enables the contactless energization and current maintainment (resistive voltage drop compensation) of superconducting magnets system**

O Tuvdensuren, H J Sung, B S Go, T T Le, M Park and I K Yu, Structural design and heat load analysis of a flux pump-based HTS module coil for a large-scale wind power generator, Journal of Physics: Conference Series, Volume 1054, (ISS2017)

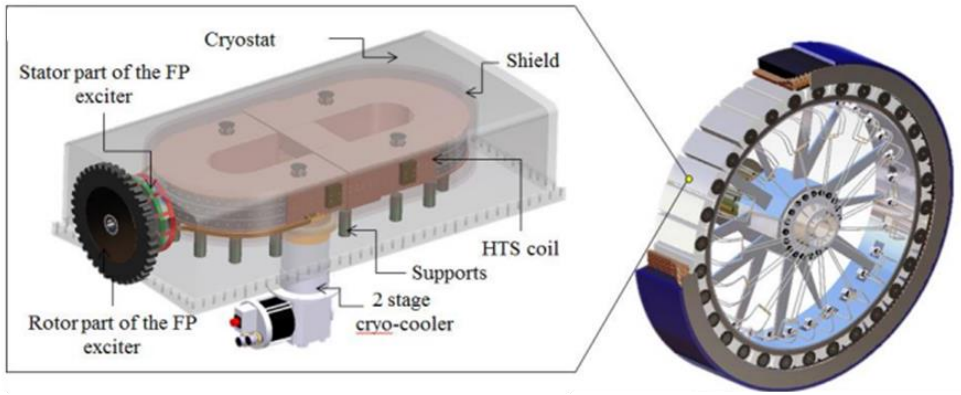

The case study

The considered flux pump consists of a 12 mm width HTS wire exposed to a rotating PM

An external two-terminal component (or load) is connected to the terminals of the HTS wire

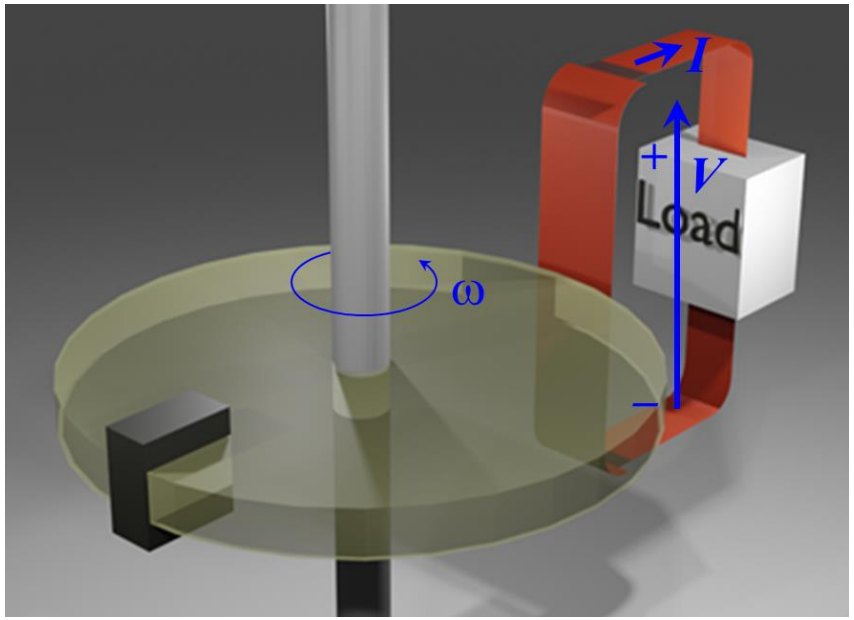

3D view of the flux pump connected to the external component.

The generator convention is assumed for the flux pump: P = V I

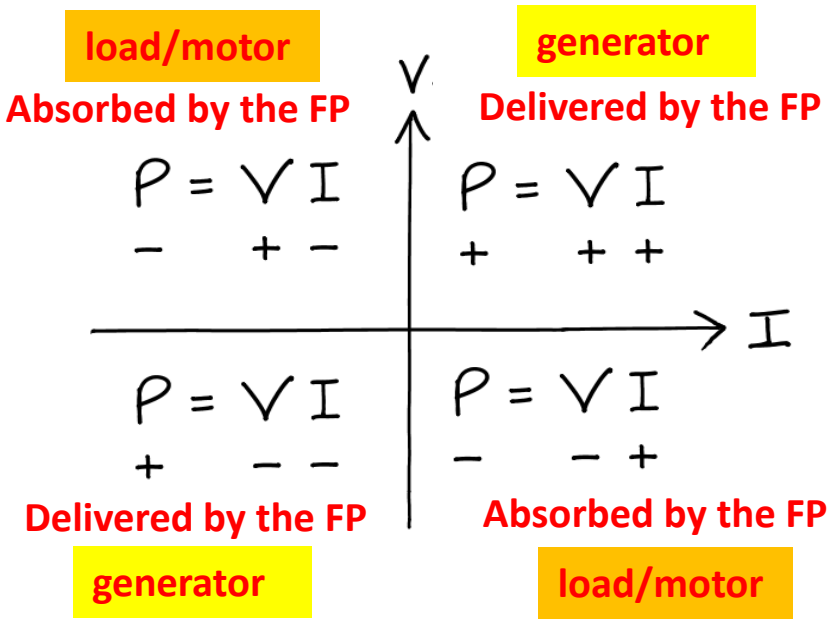

Simulated operating conditions:

Current driven (ideal current source)

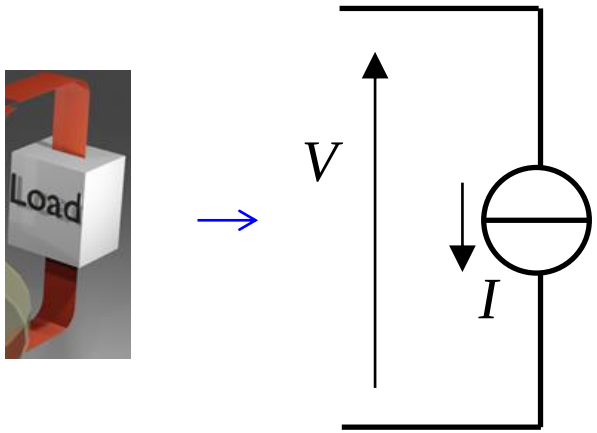

I = 0
open circuit
operation of
the FP

RL load

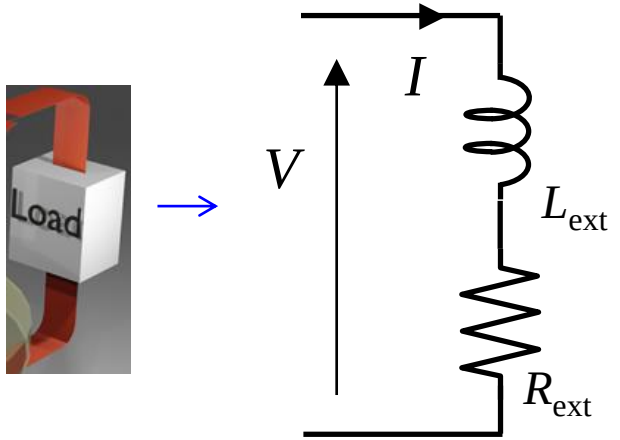

L_{ext} = 0
R_{ext} = 0
short circuit
operation of
the FP

HTS dynamo parameters

Width of the PM, a^{PM}	6 mm
Height of the PM, b^{PM}	12 mm
Depth of the PM, l^{PM}	12.7 mm
Remanence of the PM, B_r	1.25 T
Width of the HTS tape, a^{tape}	12 mm
Thickness of the HTS layer, b^{HTS}	1 μm
Critical current (77 K, self-field), I_c	283 A
n value	20
External radius of the rotor, R^{rotor}	35 mm
Air gap between the PM and the HTS tape, δ	3.7 mm
Frequency of rotation of the PM, f	25 Hz
Angular velocity of the PM, ω	(1500 rpm)
	157.08 rad s^{-1}

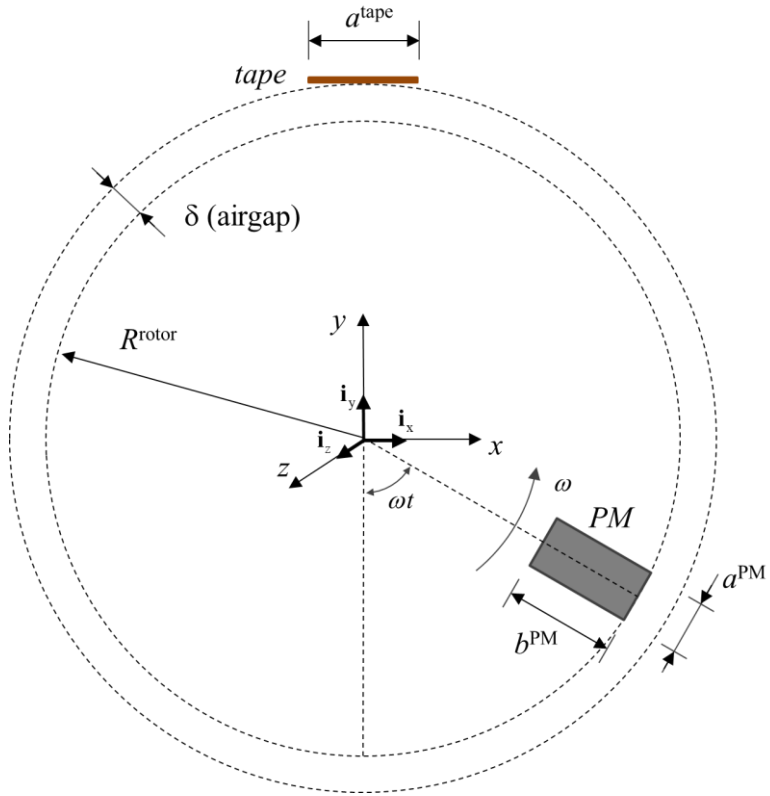

Schematic 2D section view of the flux pump

Same geometry and data as in *M. Ainslie, et al. «A new benchmark problem for electromagnetic modelling of superconductors: the high-Tc superconducting dynamo,» Superconductor Science and Technology, August 2020.*

- **A constant critical current density Jc, independent of the magnetic field B, is considered ([14], [19])**
- **The dependence of Jc on B may significantly improve the performance of the flux pump, though leaving the general trends and findings unchanged ([13], [15], [18], [20])**

Outline

- Motivation and case study
  - ✓ Geometric parameters, assumptions, types of load
- **The FEM model of the FP based on the Volume Integral Equations approach**
  - ✓ **Discretization and solving system, FEM based equivalent circuit, Energy balance and efficiency**
- Numerical results, equivalent circuits and their limits
  - ✓ Operation with impressed DC current – V-I characteristic and energy balance
  - ✓ Partial and complete equivalent circuit
  - ✓ Static and transient analysis (charging of RL load)
- Conclusion

The FEM model of the FP based on the Volume Integral Equations (VIE) approach

- **Faraday's for moving field**

$$\mathbf{E} = -\frac{\partial \mathbf{A}^{\mathrm{J}}}{\partial t} - \mathbf{v}\times\mathbf{B}^{\mathrm{PM}} - \nabla\varphi$$

(term $\boldsymbol{v}\times\boldsymbol{B}^{\mathrm{PM}}$ is equivalent to $\partial\boldsymbol{A}^{\mathrm{PM}}/\partial t$ used in other numerical approaches)

- **Ends effects are neglected - 2D Cartesian approximation is exploited**
- **The HTS layer is divided in a finite number of rectangular elements. The effect of substrate and shunt materials the tape are neglected**
- **The E-J power law is assumed for modeling the superconductor**

$$\rho(J)J = -\frac{\partial A^{\mathrm{J}}}{\partial t} - \omega\mathbf{r}\cdot\mathbf{B}^{\mathrm{PM}} - \nabla\varphi$$

$$\text{with}\quad \rho(J) = \frac{E_0}{J_{\mathrm{c}}}\left(\frac{J}{J_{\mathrm{c}}}\right)^{n-1}$$

- **The usual weighted residual approach is used for obtaining the finite dimensional solution:**

$$\int_S w_h(\mathbf{r})\left(\begin{array}{l}\rho(J)J(\mathbf{r}) + \omega\mathbf{r}\cdot\mathbf{B}^{\mathrm{PM}} + \\ + \dfrac{\mu_0}{4\pi}\displaystyle\int_S \frac{\partial J(\mathbf{r}')}{\partial \mathrm{t}}\,\Gamma(\mathbf{r},\mathbf{r}')\,dS' + v\end{array}\right)dS = 0$$

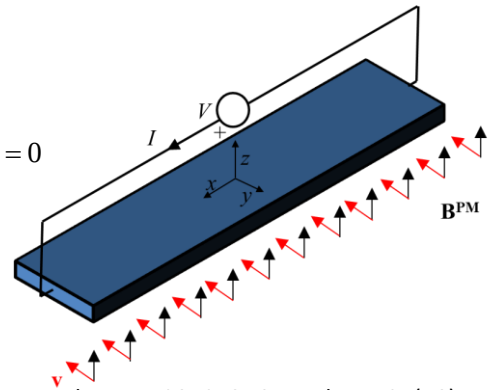

Solving system (undetermined)

$$\mathbf{M}\frac{d}{dt}\mathbf{I}_{\mathrm{w}} = -\mathbf{R}\,\mathbf{I}_{\mathrm{w}} - \mathbf{U} - \mathbf{1}\frac{V}{l^{PM}}$$

Unknowns:

- currents $\mathbf{I}_{\mathrm{w}}$ of the wires of the subdivision
- voltage *V* across the flux pump

with

$$m_{hk} = \frac{\mu_0}{4\pi}\int_{S_h}\int_{S_k}\ln\frac{1}{|\mathbf{r}-\mathbf{r}'|^2}\,dS'\,dS$$

$$r_{hh} = \rho\left(\frac{I_h}{S_h}\right)\frac{1}{S_h},\quad r_{hh} = 0 \quad \text{if} \quad h \neq k$$

$$u_h = -\omega\frac{1}{S_h}\int_{S_h}\mathbf{r}\cdot\mathbf{B}^{\mathrm{PM}}\,dS$$

A. Morandi, «2D electromagnetic modelling of superconductors, 2012, SUST, Volume 25(10)

A. Morandi and M. Fabbri, «A unified approach to the power law and the critical state modeling of superconductors in 2D», 2015, SUST 28(2)

Finite element based equivalent circuit of the flux pump

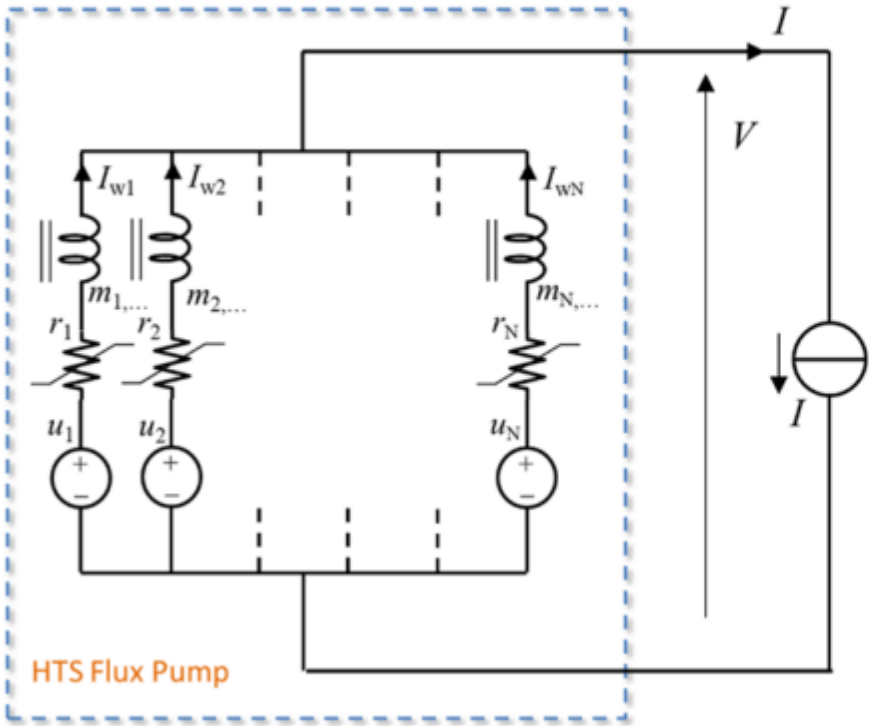

(a) connected to a current source

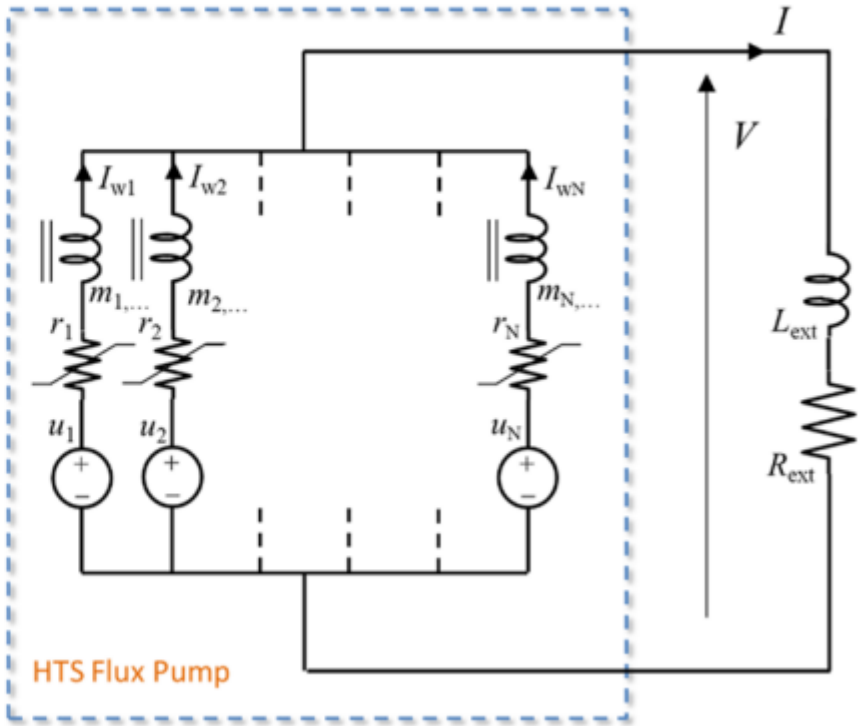

(b) connected to an RL load

Determined solving system

$$\begin{cases} \mathbf{M}\dfrac{d}{dt}\mathbf{I}_w = -\mathbf{R}\,\mathbf{I}_w - \mathbf{U} - \mathbf{1}\dfrac{V}{l^{PM}} \\ \mathbf{1}^t\ \mathbf{I}_w = I \end{cases}$$

Assigned current of the FP

Algebraic-differential

$$\begin{cases} \mathbf{M}\dfrac{d}{dt}\mathbf{I}_w = -\mathbf{R}\,\mathbf{I}_w - \mathbf{U} - \mathbf{1}\dfrac{V}{l^{PM}} \\ V = R_{ext}\,I + L_{ext}\dfrac{d}{dt}I \end{cases}$$

Differential link btw voltage and current of the FP

Differential

Energy Balance

$$\rho J\,\mathbf{i}_z = -\frac{\partial A^J\,\mathbf{i}_z}{\partial t} - (\omega \mathbf{i}_z \times \mathbf{r}) \times \mathbf{B}^{PM} - \nabla\varphi\,\mathbf{i}_z$$

$$\rightarrow \rho J^2 = -\frac{\partial}{\partial t}\left(\frac{1}{2} J A^J\right) - \left(J\,\mathbf{i}_z \times \mathbf{B}^{PM}\right) \times \mathbf{r} \cdot \omega \mathbf{i}_z - J\nabla\varphi$$

$$\rightarrow -\omega l^{PM} \int_S \left(J\,\mathbf{i}_z \times \mathbf{B}^{PM}\right) \times \mathbf{r}\,dS = V I + l^{PM} \int_S \rho J^2\,dS + l^{PM} \frac{\partial}{\partial t} \int_S \frac{1}{2} J A^J\,dS$$

discrete equivalent

$$\omega l^{PM} \sum_h I_h \left(x_h B^{PM}_{x,h} + y_h B^{PM}_{y,h} \right) = V I + \sum_h \rho_h \frac{l^{PM}}{S} I_h^2 + \frac{d}{dt}\left(l^{PM} \frac{1}{2} \sum_h \sum_k m_{hk} I_h I_k \right)$$

Instant energy balance of the Flux pump

$$-T\omega \quad = \quad V I \quad + \quad P_J \quad + \quad \underbrace{\frac{d}{dt} W_{mag}}$$

Mechanical power supplied to the rotor

Electric power delivered to the load

dissipated power

Change of magnetic energy

with $T = l^{PM} \int_S \left(J\,\mathbf{i}_z \times \mathbf{B}^{PM}\right) \times \mathbf{r}\,dS$

Mechanical torque of the rotor

Energy balance in one cycle

$$\underbrace{-\int_t^{t+T} \omega T\,dt'}_{E_{mech}} = \underbrace{\int_t^{t+T} VI\,dt'}_{E} + \underbrace{\int_t^{t+T} \omega T\,dt'}_{E_{joule}}$$

E_{mech}, mechanical energy supplied to the rotor

E, Electric energy delivered to the load

E_{joule}, disspitaed energy

Cycle efficiency of the flux pump

$$\eta = \frac{E}{E_{mechanical}} = \frac{E}{E + E_{joule}}$$

Outline

- Motivation and case study
  - ✓ Geometric parameters, assumptions, types of load
- The FEM model of the FP based on the Volume Integral Equations approach
  - ✓ Discretization and solving system, FEM based equivalent circuit, Energy balance and efficiency
- **Numerical results, equivalent circuits and their limits**
  - ✓ **Operation with impressed DC current – V-I characteristic and energy balance**
  - ✓ Partial and complete equivalent circuit
  - ✓ Static and transient analysis (charging of RL load)
- Conclusion

Numerical results / electromotive force $(v \times B^{\mathrm{PM}})$ in one cycle

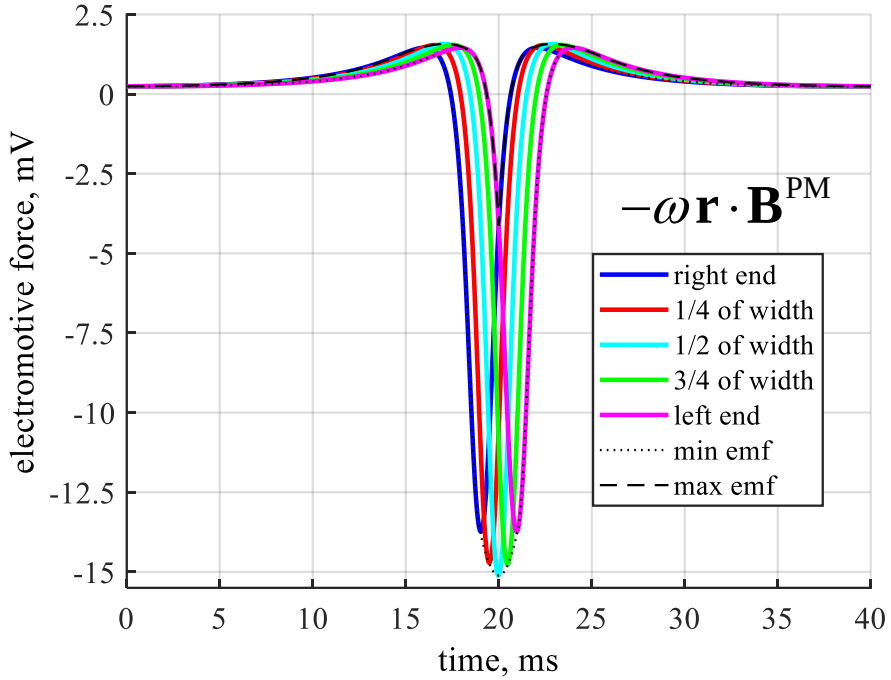

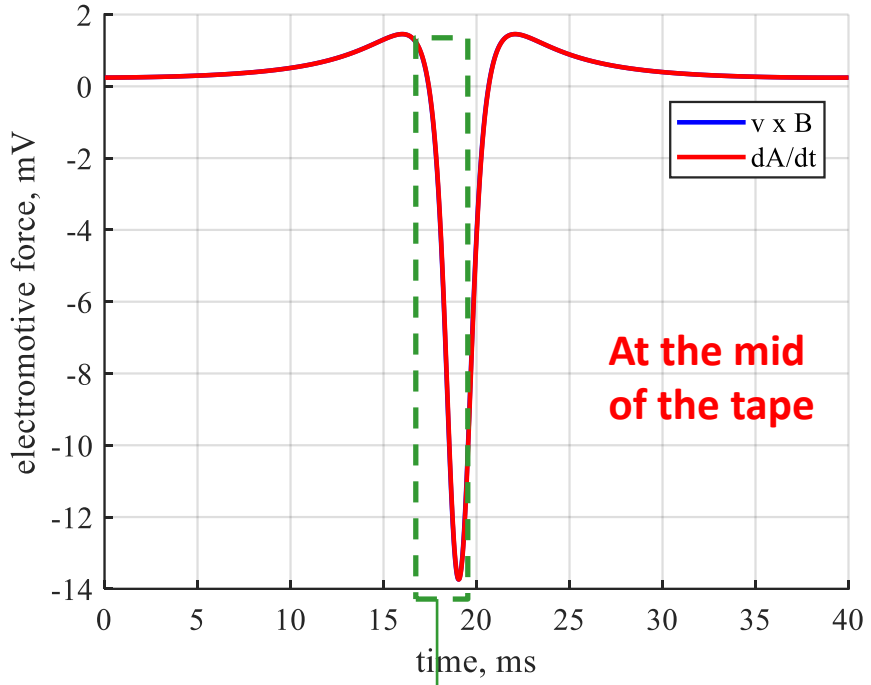

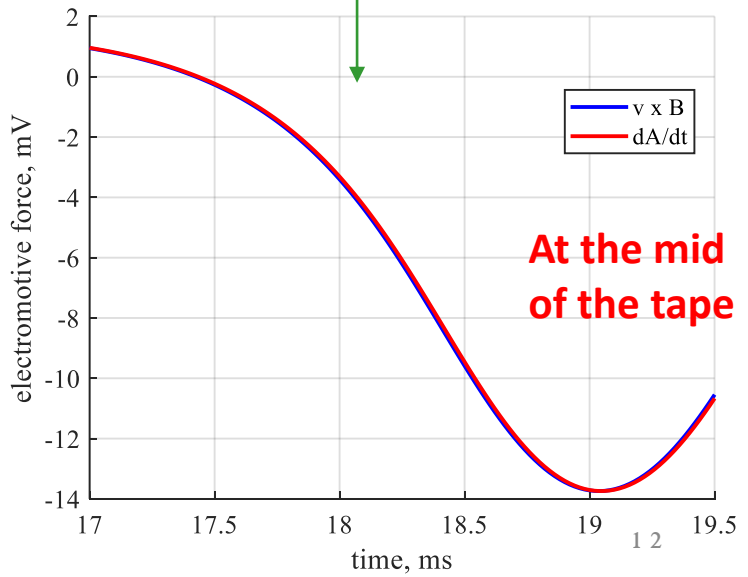

- electromotive force $v \times B^{\mathrm{PM}}$ has zero average at all points and reaches about 150 mV peak at the middle of the tape
- term $v \times B^{\mathrm{PM}}$ is coincident with $\partial A^{\mathrm{PM}}/\partial t$ evaluated via numerical derivative

Numerical results / Terminal voltage of the FP at various impressed DC currents

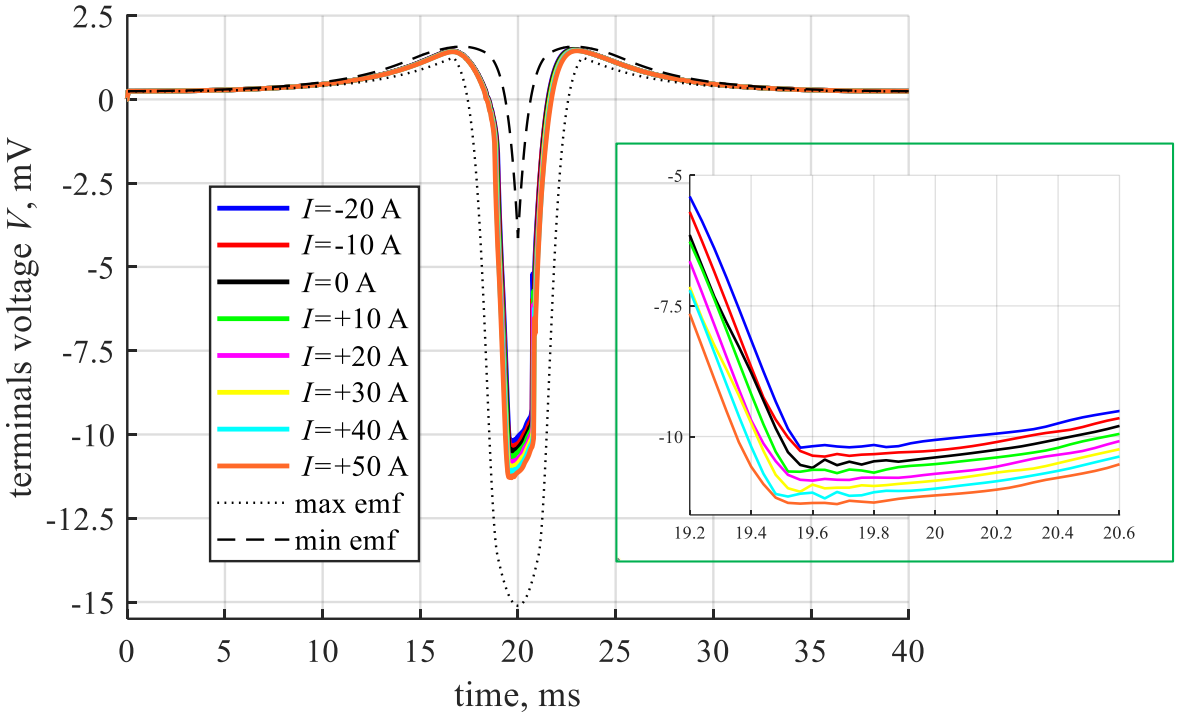

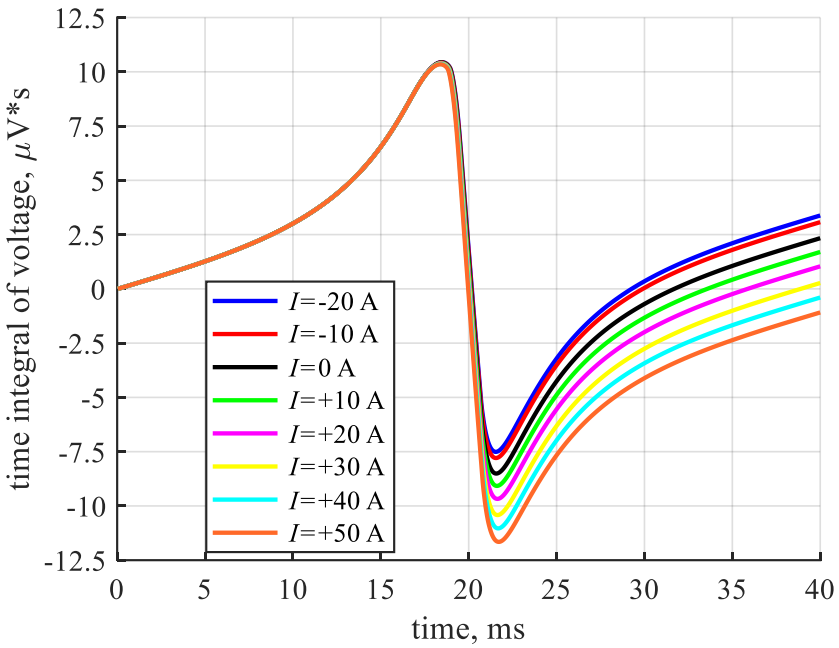

- **At all impressed currents, the terminal voltage is comprised between the min. and max. emf at any instant**
- **The voltage has non-zero DC component in one cycle, as a result of the distributed emf combined with the non-linear resistivity of the HTS**
- **The DC voltage can be positive or negative depending on the DC current. A monotone decrease of the voltage with increasing current is observed at all instants. As a result, a monotone decrease of the DC voltage with the impressed current is obtained**

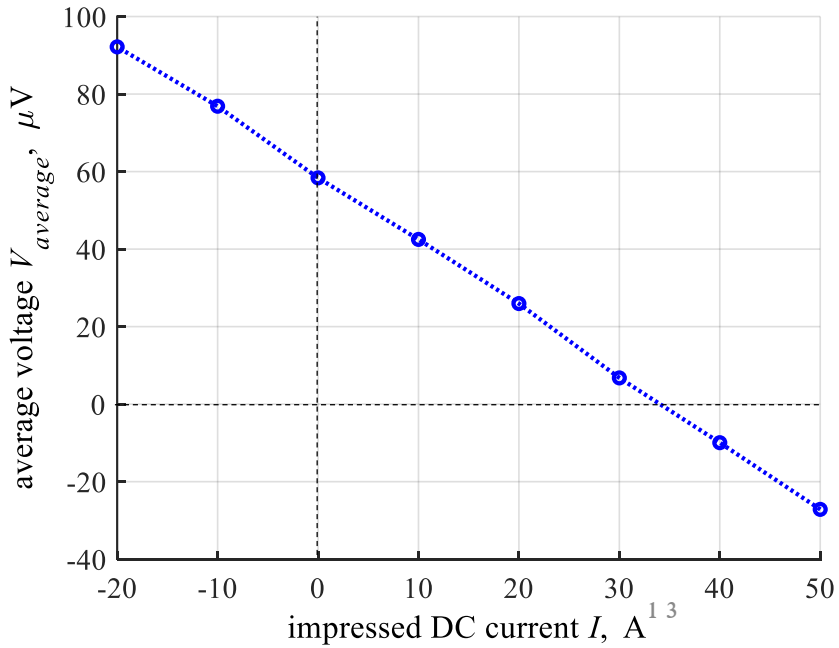

Numerical results / Effect of rotation and V_{dc}-I_{dc} characteristic of the flux pump

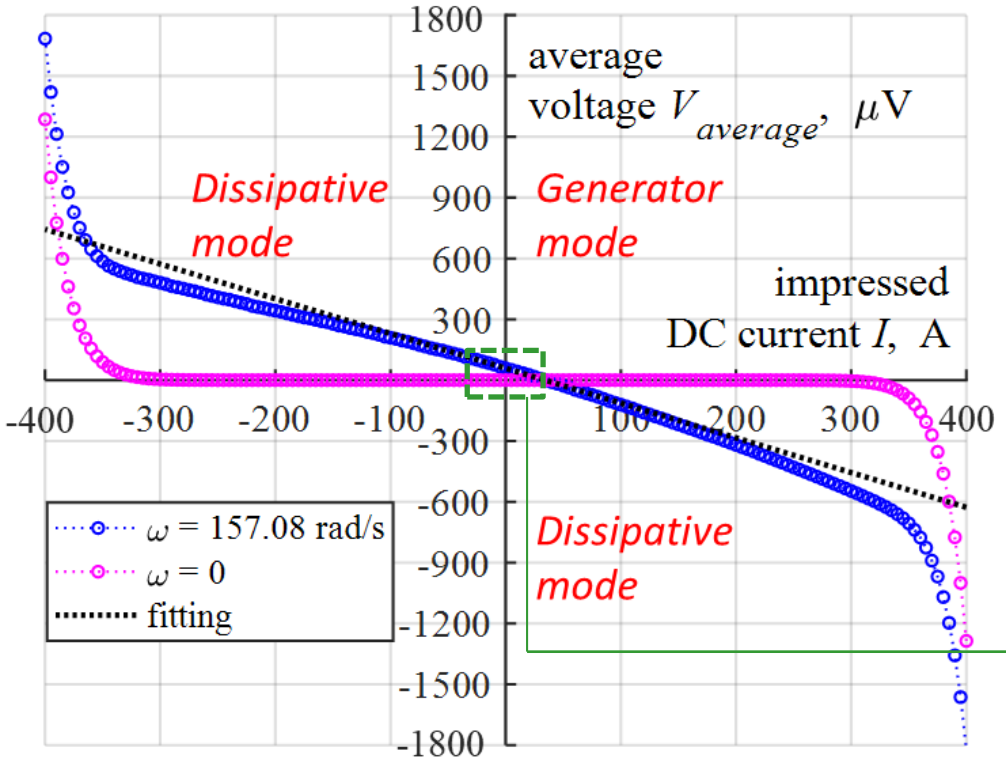

The effects of the rotation are:

- **Shifting the VI curve into the first quadrant allowing power generation**
- **Increasing the power to be supplied for impressing a DC current out of the generation mode (power must be supplied which is converted, along with th mechanical one, in AC loss into the tape)**

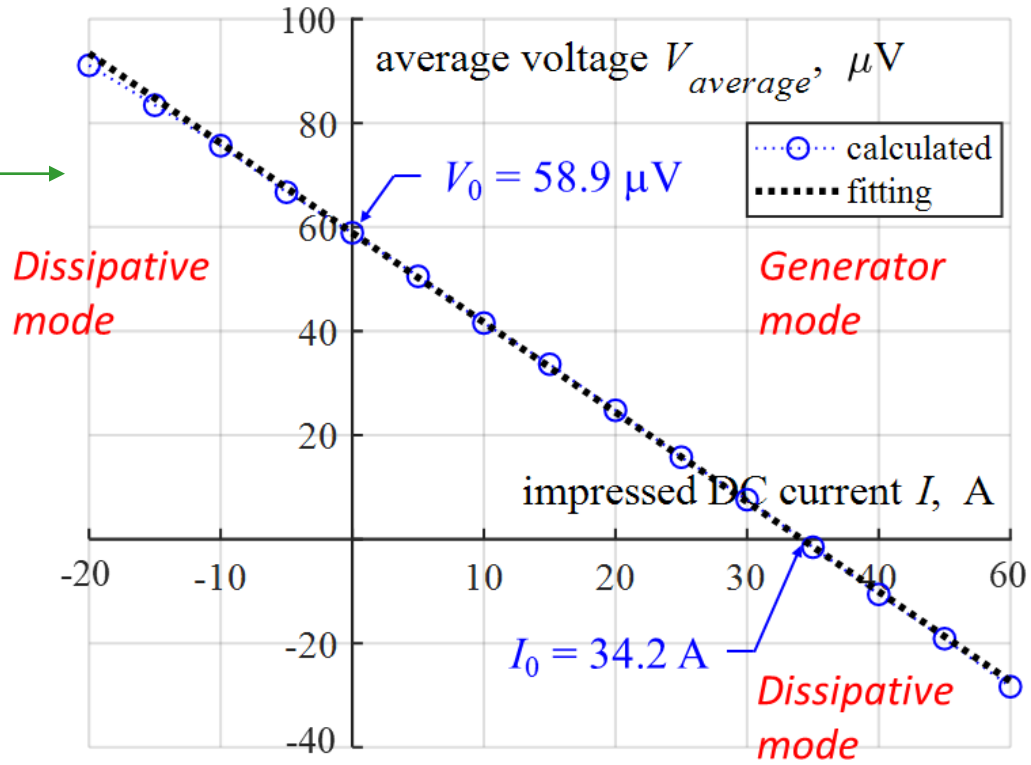

- **The maximum current I_0 (34.2 A) for which power generation is possible is much lower than the critical current I_c of the tape (283 A).**
- **Supplying power to a load requiring a current greater than I_0 is not possible. For fixed air gap and angular velocity, I_0 is an intrinsic parameter of the flux pump and does not depend on the load connects to it.**

Numerical results / Energy balance

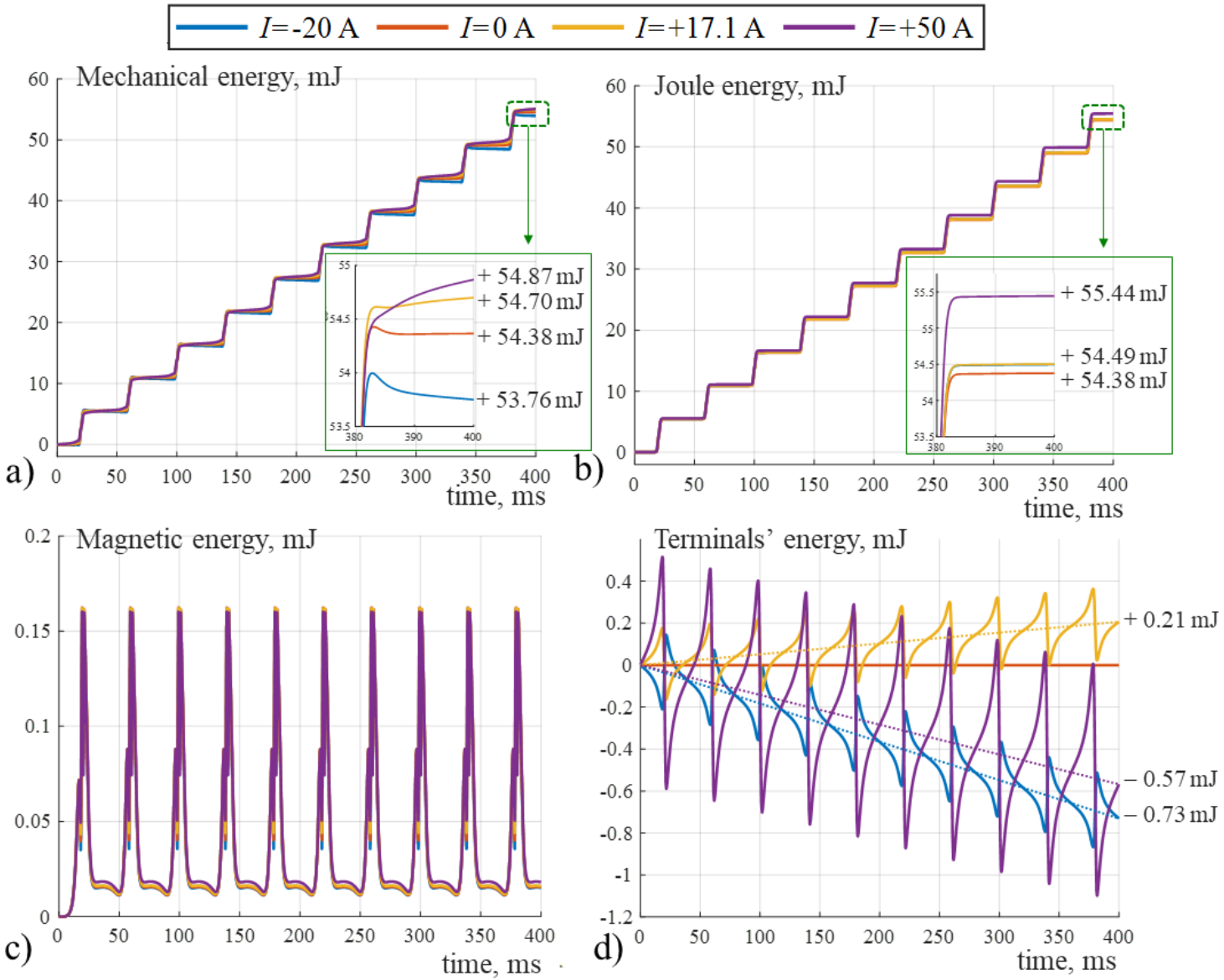

Energy terms of the flux pump during ten cycles for different DC current

- **Monotone trends (unidirectional transfer) are observed for mechanical energy, dissipated energy and energy exchanged with the external component**
- **Mechanical energy is always positive. No energy can be extracted from the rotor (motor behavior).**
- **The energy transferred to the external components can be both positive or negative (generator or the dissipative mode), depending on the DC current. In dissipative mode the energy absorbed by the external component is converted, along with the mechanical energy of the rotor, into heat**
- **Energy exchanged with the external component is much lower than the dissipation**

Average power in one cycle for different values of the DC impressed current and corresponding efficiency

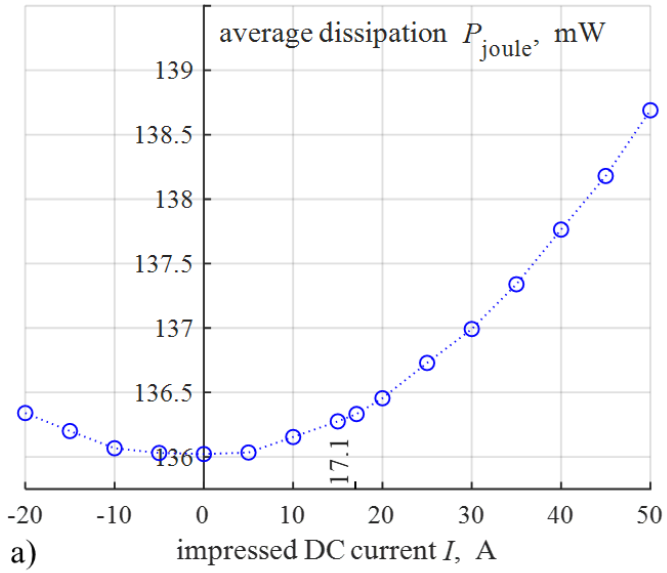

a)

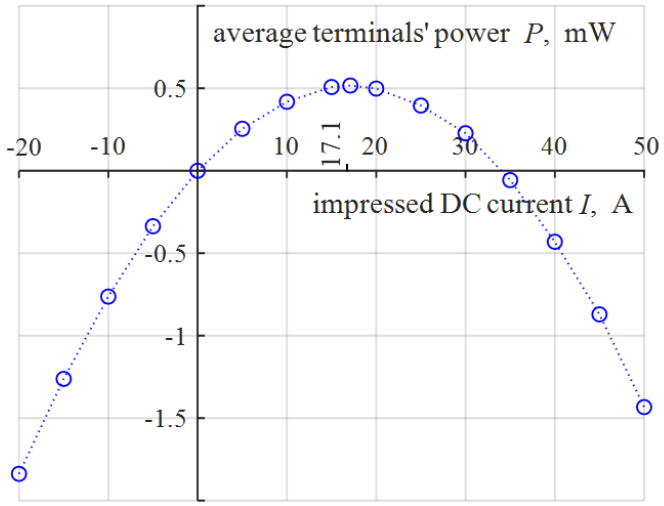

b)

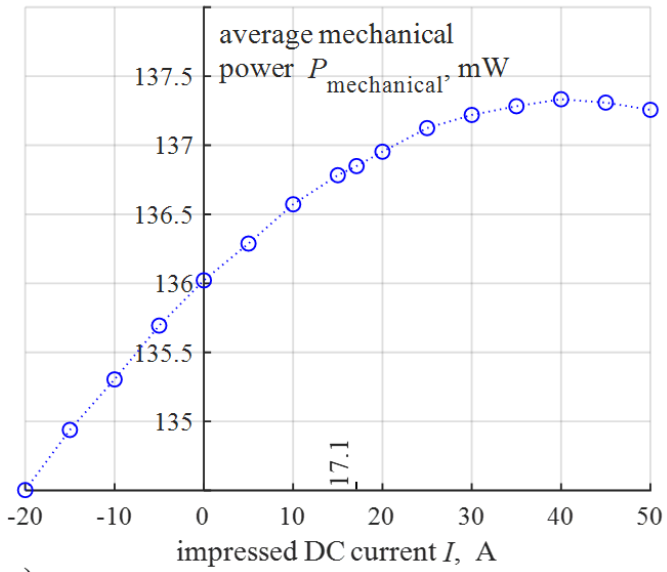

c)

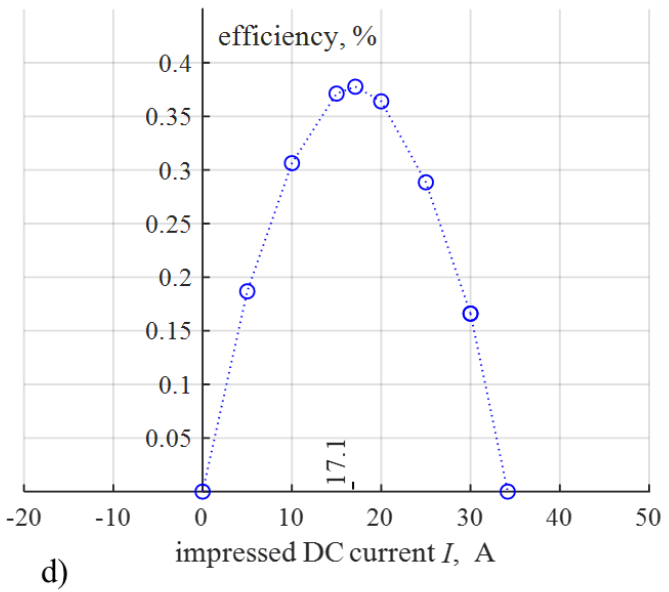

d)

- **A positive average power is delivered to the external component in the range [0 – I_0].**
- **The mechanical power is always positive. The flux pump only never acts in the motor mode.**
- **Only a small part of the mechanical power is transferred to the external load. This is due to the inherent dissipation associated with the induced current, responsible for the DC voltage, occurring also in no load conditions.**
- **As a result, a maximum efficiency of 0.39% is reached at 17.1 A (I_0 /2).**

It must be reminded that accounting for the dependence of Jc on the *B* field improveds the absolute performance f the FP, while leaving all presnete conclusion and tresnds uncehanged.

Outline

- Motivation and case study
  - ✓ Geometric parameters, assumptions, types of load
- The FEM model of the FP based on the Volume Integral Equations approach
  - ✓ Discretization and solving system, FEM based equivalent circuit, Energy balance and efficiency
- Numerical results, equivalent circuits and their limits
  - ✓ Operation with impressed DC current – V-I characteristic and energy balance
  - ✓ **Partial and complete equivalent circuit**
  - ✓ **Static and transient analysis (charging of RL load)**
- Conclusion

Partial and complete empirical equivalent circuits

- **A monotone decrease of the voltage with increasing current is observed at all instants**

$$V(t,I) = V(t,0) - R(t,I)\,I$$

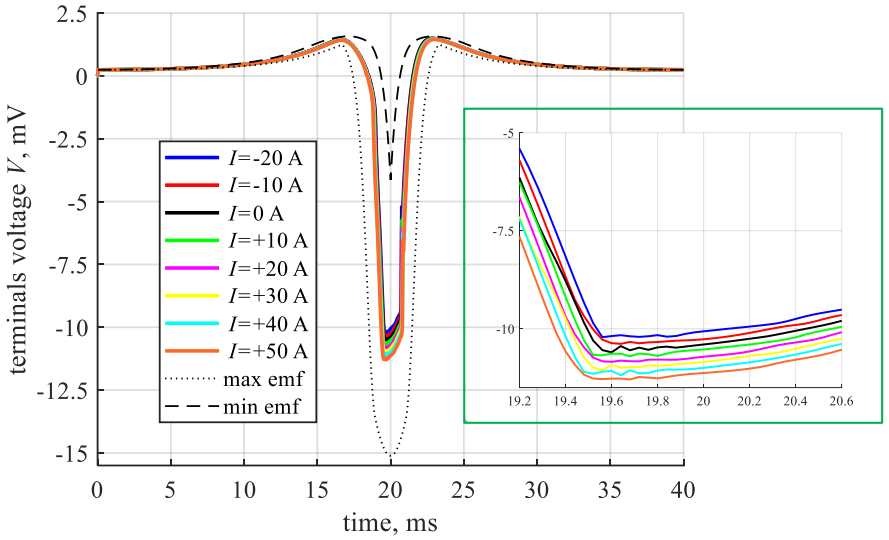

- **A linear decrease, confirmed in experiments, of the average terminal voltage on the operating current in the interval ±100 A**

$$V_{\text{average}}(I) = V_0 - R_{\text{effective}}\,I$$

$$R_{\text{effective}} = \frac{V_0}{I_0}, \quad \text{independent on } I$$

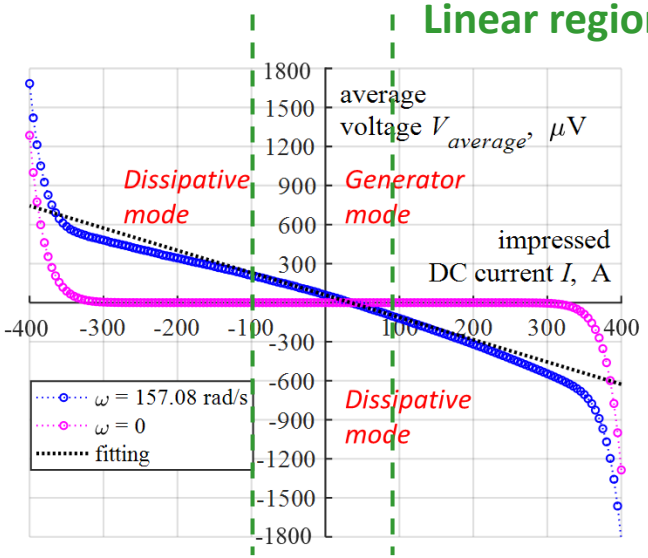

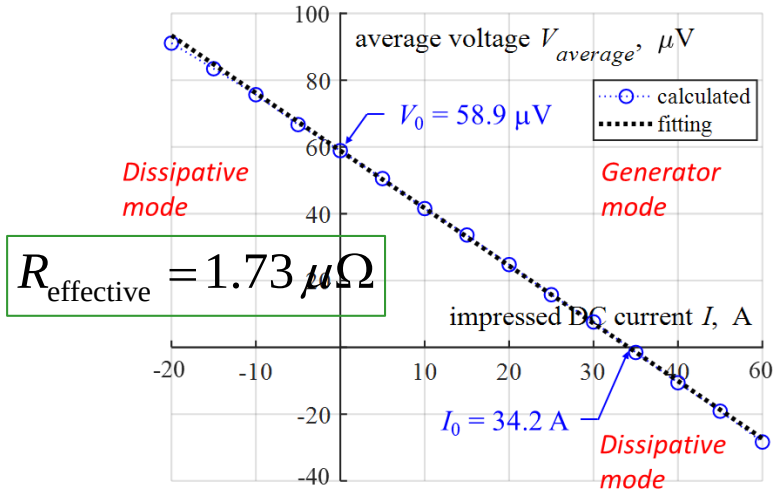

- **We assume that, provided that the current *I* is in the linear interval ±100 A, the constant effective resistance $R_{effective}$ determines the difference between the instantaneous terminal voltage and the no load voltage**

$$V(t,I) = V(t,0) - R(t,I)\,I$$

$$V(t,I) = V(t,0) - R_{\text{effective}}\,I$$

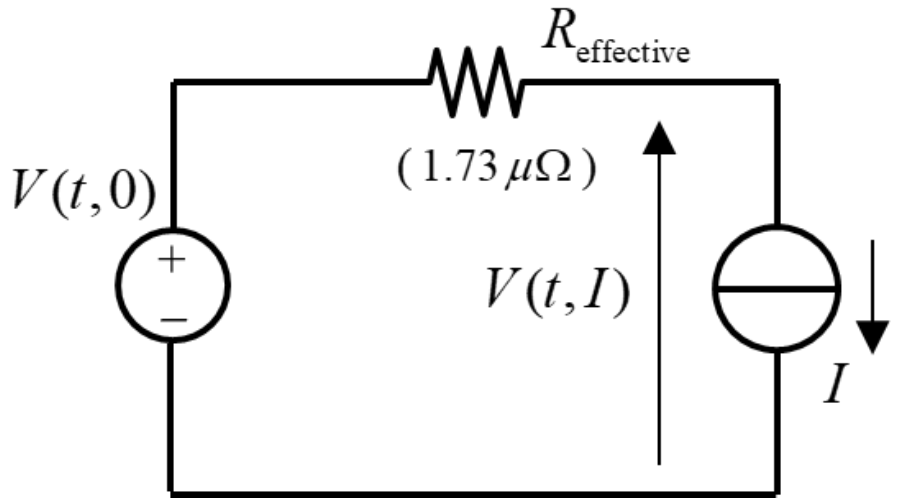

partial empirical equivalent circuit of the flux pump

A TIME DEPENDENT CIRCUIT ALLOWING TRANSIENT SIMULATIONS

- **Replacing R(t,I) with a constant $R_{effective}$ is a merely heuristic assumption, validated by comparison with FEM results**

- **It is pointed out that the equivalent circuit is supplied by the time dependent open circuit voltage V(t,0) and not by the open circuit voltage $V_{average}$ as it is usually assumed**

- **The partial equivalent circuit is not able to reproduce the dissipation that occurs in case of open circuit operation**
- **An intrinsic resistance must be added to take this dissipation into account**

$$P_{joule0} = \frac{\int_{t}^{t+T} \frac{V^2(t,0)}{R_{intrinsic}} dt'}{T} \longrightarrow R_{intrinsic} = \frac{V_{rms0}^2}{P_{joule0}} \longrightarrow$$

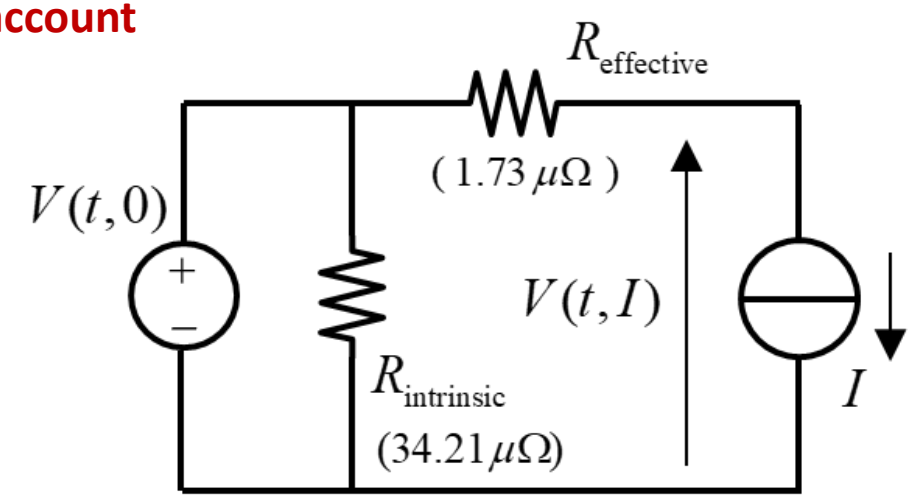

complete empirical equivalent circuit of the flux pump

A TIME DEPENDENT CIRCUIT ALLOWING TRANSIENT SIMULATIONS AND TAKING LOSS INTO ACCOUNT

- **The Thevenin equivalent of the complete empirical equivalent circuit coincides with the partial one (they are distinguishable from the external load)**
- **Both the partial and complete empirical equivalent circuits can be equivalently used for time domain analysis, provided that the linear limit is not exceeded. The complete equivalent circuit must be used for taking the loss into account.**

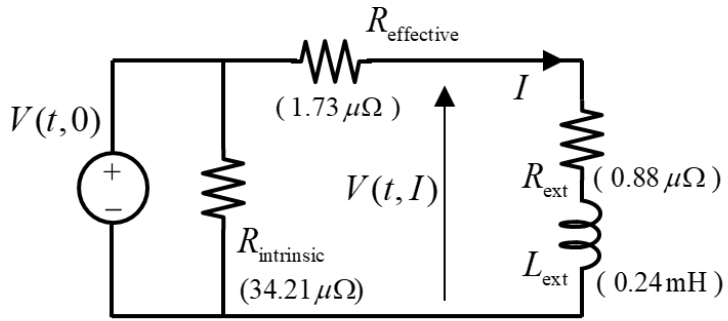

a)

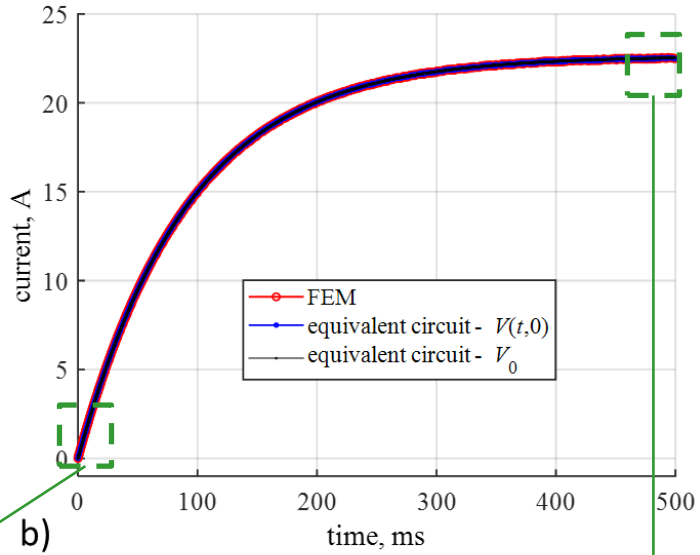

b)

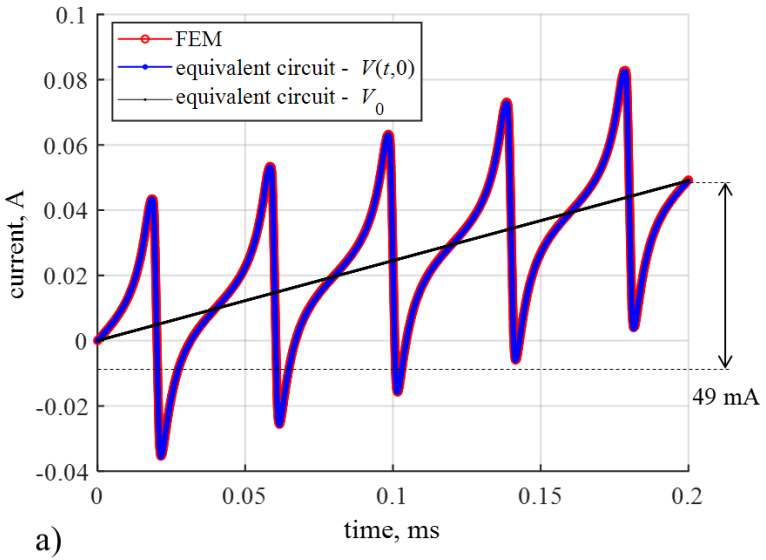

a)

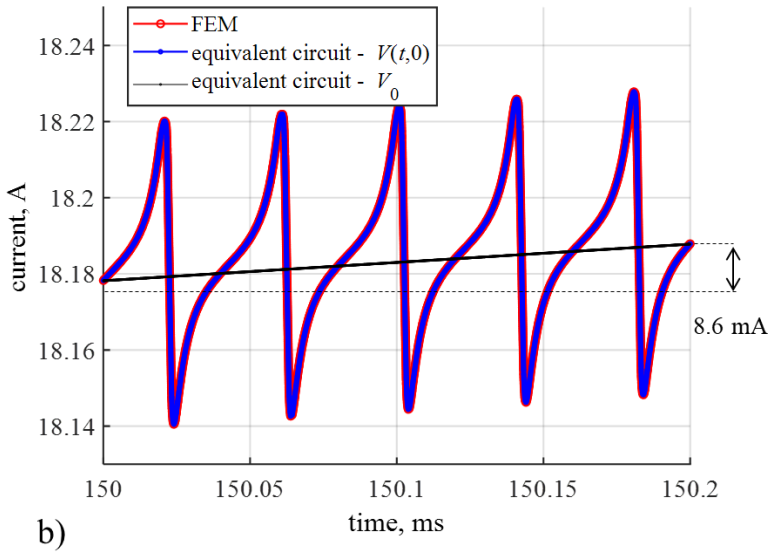

b)

- **The current ripple during the whole charging is accurately calculated by means of the equivalent circuit**
- **The flux pump is completely characterized by means of:**
  - **V(t,0)**
  - **$R_{effective}$**
  - **$R_{intrinsic}$**
- **Once these parameters are defined any simulation can be accomplished provided that the linear limit is not is not exceeded**

RL load charging transient calculated by means of the equivalent circuit

Terminology: “short circuit operation” versus “current producing zero average voltage at the terminals”

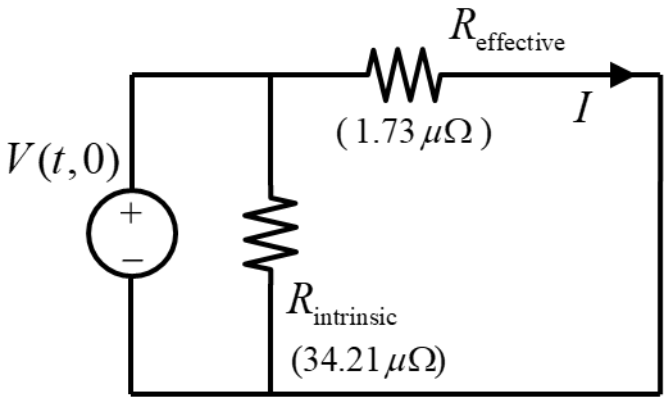

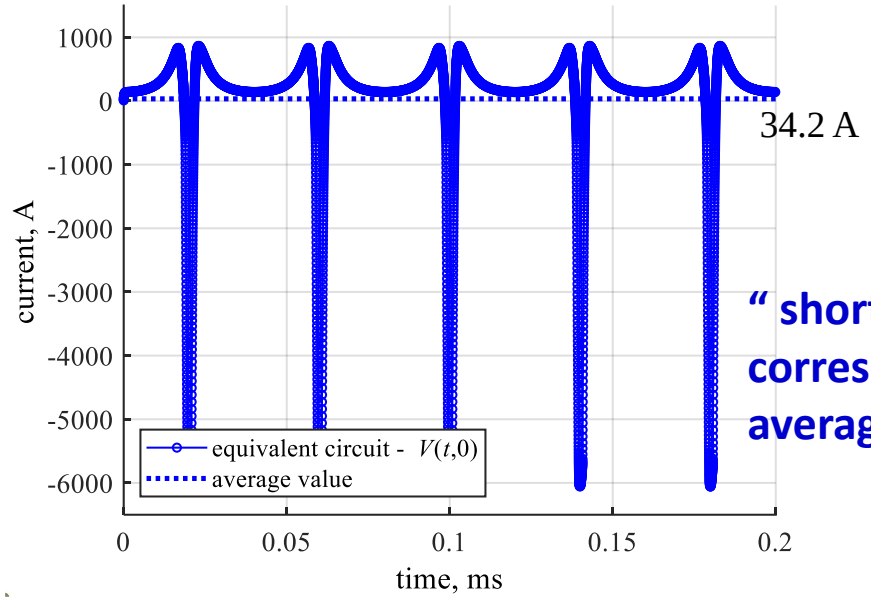

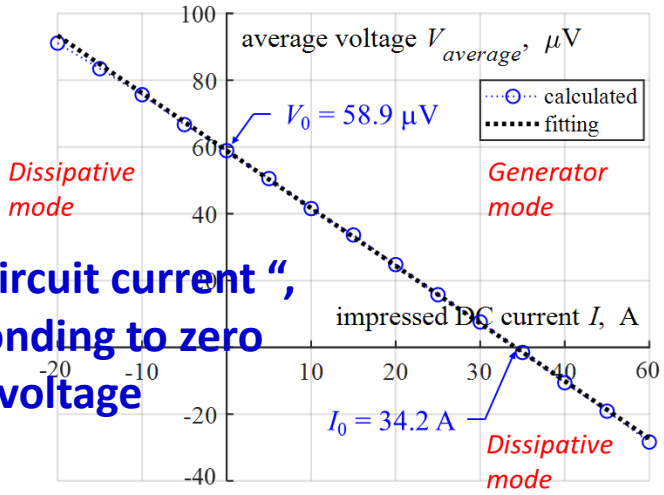

“ short circuit current “, corresponding to zero average voltage

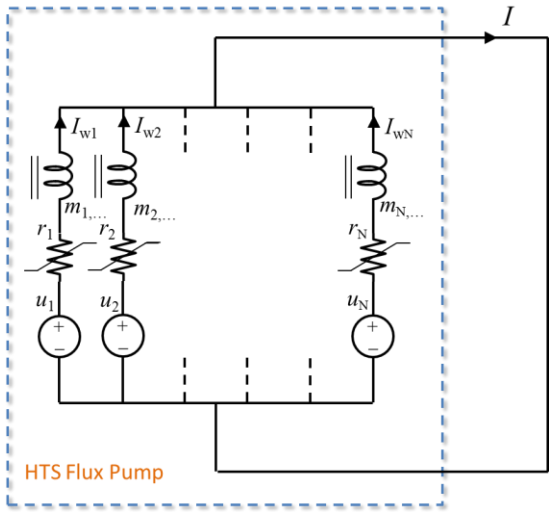

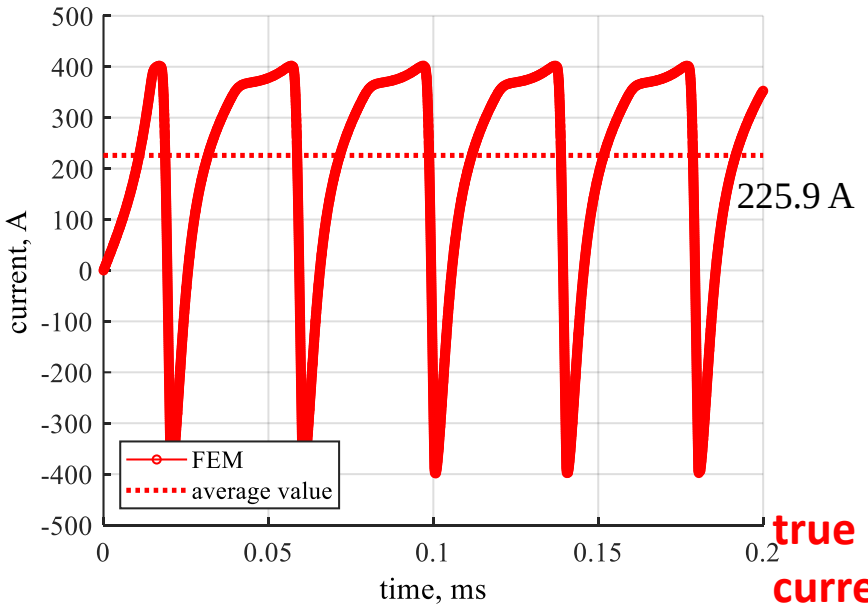

- **The short circuit current is beyond the linear limit and cannot be calculated by means of the equivalent circuit. The FEM model is needed.**

true “short circuit current “

Energy behavior: Average power in a cycle for different values of DC current and corresponding efficiency

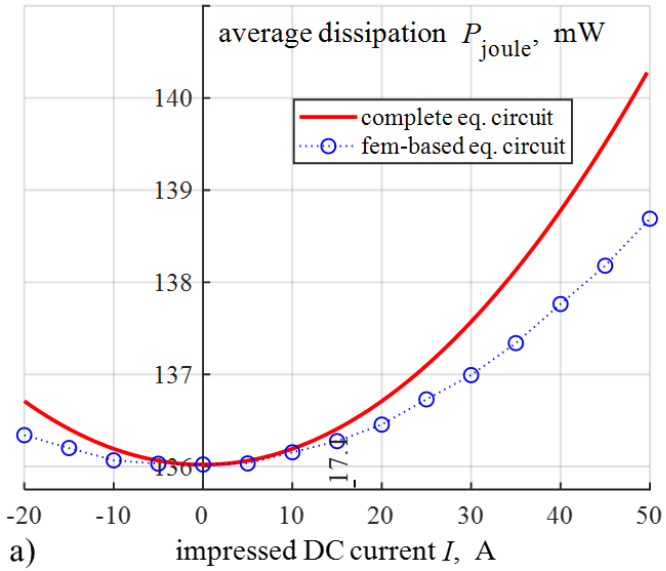

a)

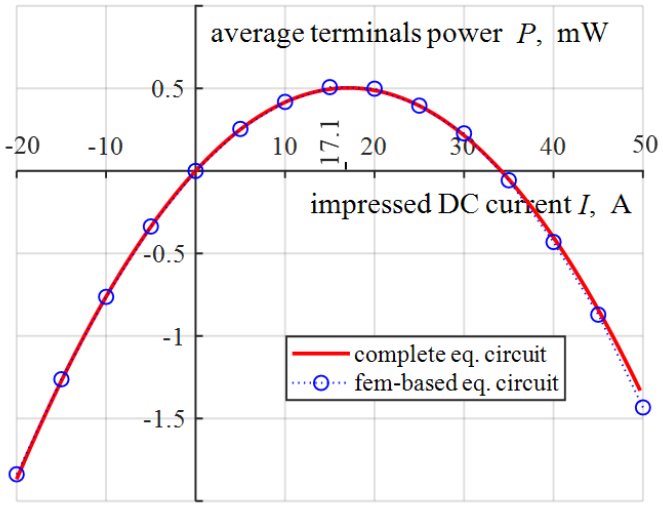

b)

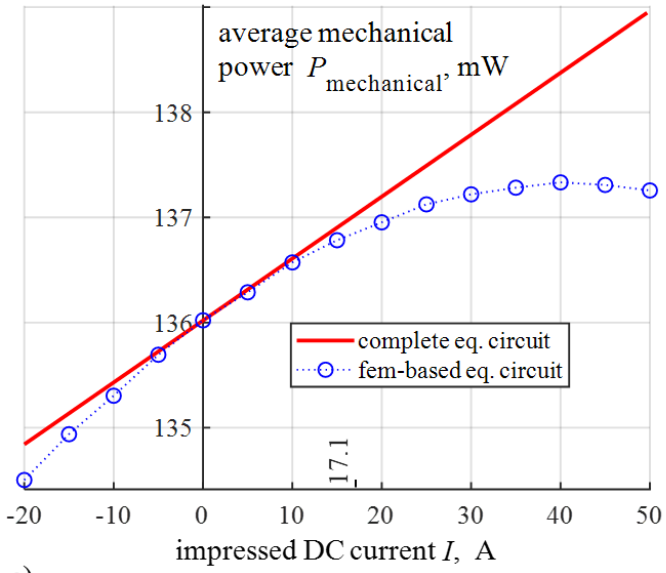

c)

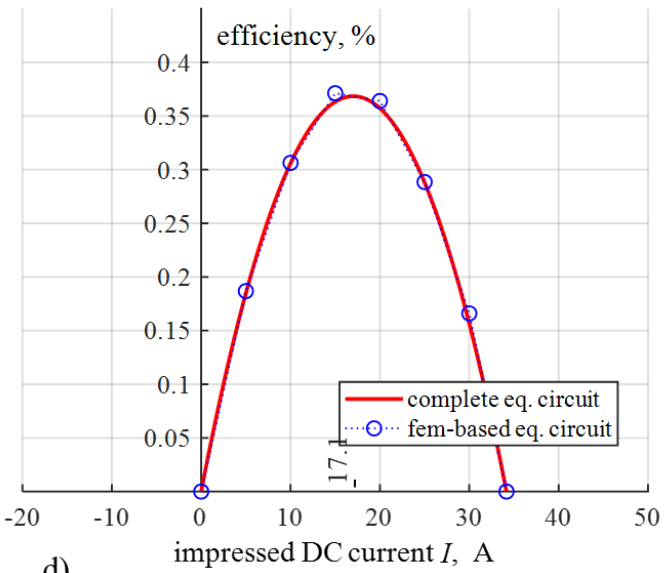

d)

$$P_{source(complete)} = V_0 I + \frac{V_{rms0}^2}{R_{intrinsic}} = VI + R_{effective} I^2 + \frac{V_{rms0}^2}{R_{intrinsic}} =$$

$$= P_{terminals} + \underbrace{R_{effective} I^2 + P_{joule0}}_{\text{overall joule dissipation}}$$

$$\eta_{(complete)} = \frac{P_{terminals}}{P_{source(complete)}} = \frac{P_{terminals}}{P_{terminals} + R_{effective} I^2 + P_{joule0}}$$

- **In agreement with experiment, the calculated average power in one cycle at the terminals follows a parabolic dependence and is maximum at $I=I_0/2$.**
- **Efficiency too is maximum at $I=I_0/2$. Flux pump should be designed to operate at this rated current**
- **A drastic increase of efficiency is obtained if the dependence of Jc on B is considered.**

Findings and conclusion

- In dynamo FP a significant part of the supplied mechanical power is inherently converted in heat due to overcritical currents induced to produce the DC voltage.
- The generator mode can only be achieved in a restricted range of current, independent on the load. In no conditions the FP can operate in motor mode.
- Maximum power transfer and efficiency are reached at the middle of the intrinsic generator range ($I_0/2$)
- An intrinsic resistance must be added to the equivalent circuit to take loss into account
- The equivalent circuit can be used for time domain simulations of any type, provided that the current is in the linear limit

antonio.morandi@unibo.it

$$\int_S w_h(\mathbf{r})\left(\rho(J)\, J(\mathbf{r}) + \omega \mathbf{r} \cdot \mathbf{B}^{\mathrm{PM}} + \frac{\mu_0}{4\pi} \int_S \frac{\partial J(\mathbf{r}')}{\partial \mathrm{t}}\ \Gamma(\mathbf{r},\mathbf{r}')\, dS' + v \right) dS = 0$$